ACS Macro Letters

Letter

pubs.acs.org/macroletters

Multistep Thickening of Nafion Thin Films in Water

Yudai Ogata,[†] Daisuke Kawaguchi,[‡] Norifumi L. Yamada,[§] and Keiji Tanaka*[,†,∥]

[†]Department of Applied Chemistry and [‡]Education Center for Global Leaders in Molecular System for Devices, Kyushu University, Fukuoka 819-0395, Japan

[§]Neutron Science Laboratory, High Energy Accelerator Research Organization, Ibaraki 319-1106, Japan

[∥]International Institute for Carbon-Neutral Energy Research (WPI-I2CNER), Kyushu University, Fukuoka 819-0395, Japan

Supporting Information

ABSTRACT: Water sorption kinetics in thin Nafion films prepared on silver and silicon oxide substrates was examined by surface plasmon resonance and neutron reflectivity measurements. It was found that the films thickened in three regimes. The asymptotic swelling ratios in regimes I, II, and III were 1.05, 1.26, and 1.41, respectively. These values were independent of the substrate species and were coincident with the transition points of different hydration states in the bulk Nafion; water binding to sulfonic acid groups, the formation of sphere-like ionic clusters, and bridge formation between clusters. The swelling was much slower in thin films than in the bulk due to the mobility restriction of Nafion near the substrate.

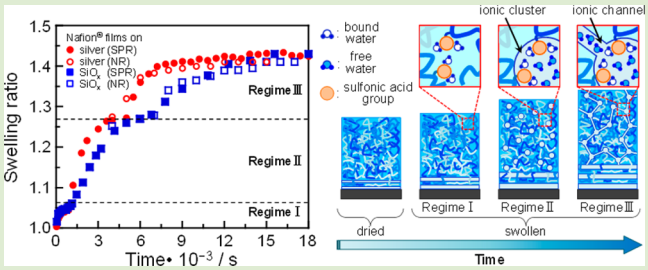

Known for its remarkable conductivity and durability, Nafion is widely used as a proton exchange film in polymer electrolyte fuel cell (PEFC).[1−3] Such excellent electrochemical and mechanical properties of Nafion are associated with the characteristic network structure of the hydrated water phase. Extensive studies have revealed that the microstructure in the Nafion film depends on the swelling ratio defined as the value of the film thickness in water divided by the original thickness.[4−9] In the case of a swelling ratio up to 1.05, water molecules strongly interact with the sulfonic acid groups of Nafion and thus bind to them.[4,5] Once the swelling ratio goes beyond 1.05, sphere-like ionic clusters evolve, induced by the sorption of water molecules that weakly interact with sulfonic acid groups compared to bound water molecules.[6,7] When the swelling ratio further increases over 1.26, the clusters become connected together through cylindrical or disordered networks of hydrophilic water domains.[8,9] However, it appears to us that most studies conducted so far in this context are limited to bulk systems. Downsizing PEFC is one of the interesting developments in the near future. Issues of portability and miniaturization without sacrificing the system efficiency are therefore important. To accept such a challenge, all components in a PEFC, including the polyelectrolyte film, should therefore become smaller and thinner.

The physical properties of a polymer film generally altered with decreasing thickness for films thinner than 100 nm.[10−14] Although the reasons how such peculiar dynamics are manifested is still controversial, the effects of air and substrate interfaces on thin films are undoubtedly responsible for this thickness dependency. Works published in the current literature have shown that chain dynamics at the air and substrate interfaces should be enhanced and depressed in comparison with that in the internal region, respectively. This is because the ratio of interfacial area to the total volume of the film increases markedly with decreasing film thickness. Actually, recent studies have demonstrated that the thickness as well as interfaces can be affected by the structure of the hydrated domain, water-vapor diffusion, and proton conductivity.[15−18]

In this study, the thickness of thin Nafion films in water was characterized as a function of time by surface plasmon resonance (SPR) reflectivity[19,20] in conjunction with neutron reflectivity (NR) measurements. Here, we show that once the thin Nafion films contact with liquid water, the thickness increases in three steps, which could be associated with the structural evolution in hydrated domains. The results presented allow us to discuss the water sorption kinetics in thin Nafion films.

Figure 1a shows a typical SPR reflectivity curve for a thin Nafion film with an original thickness (h_0) of 47 nm. The substrate used was a silver-deposited glass because the metal coating was necessary to generate SPR and was a model electrode. The surface of the Nafion film was sufficiently flat to be characterized by SPR (Figure S1 of the Supporting Information). The refractive indices of Nafion and water are 1.35 and 1.33, respectively. Thus, as long as the substrate is well characterized, the SPR reflectivity curve is almost determined only by the thickness of the Nafion film. A simulation based on a transfer matrix method enables us to determine the thickness of the film in water.[21] The solid curve in Figure 1a is the best-fit reflectivity to the experimental result.

Received: June 20, 2013
Accepted: September 10, 2013
Published: September 13, 2013

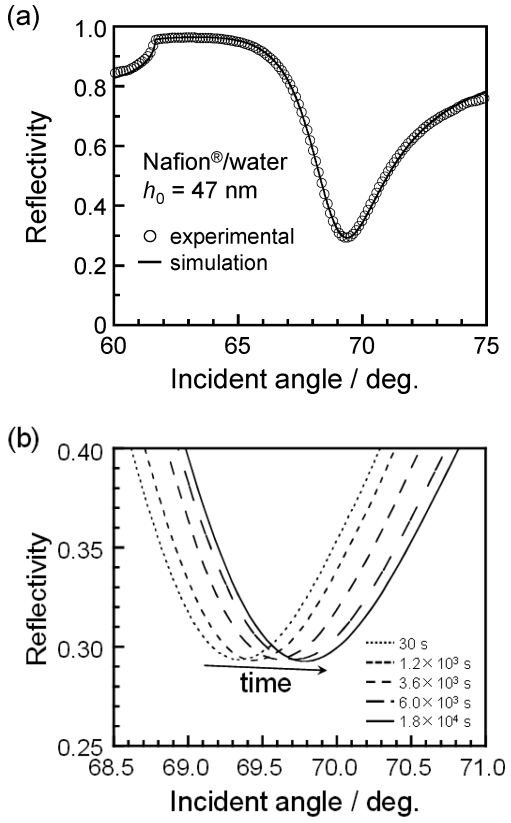

Figure 1. (a) SPR reflectivity curve for a Nafion film with an original thickness (h_0) of 47 nm in water. Open symbols and solid line denote experimental and calculated reflectivity, respectively. (b) Time course of a typical SPR reflectivity curve for the Nafion film contacting water.

Figure 1b shows the time course of the reflectivity curve for the 47 nm thick Nafion film after contacting with water. In the reflectivity curve, the resonance angle was shifted to the higher angle side. Fitting the experimental reflectivity reveals that the Nafion film became thicker with time due to the water sorption.

Figure 2 shows the time dependence of the swelling ratio for Nafion films on silver and SiO_x substrates, respectively, after coming in contact with water. The SiO_x substrate was prepared by the sputter-coating of SiO_x onto the silver substrate. The

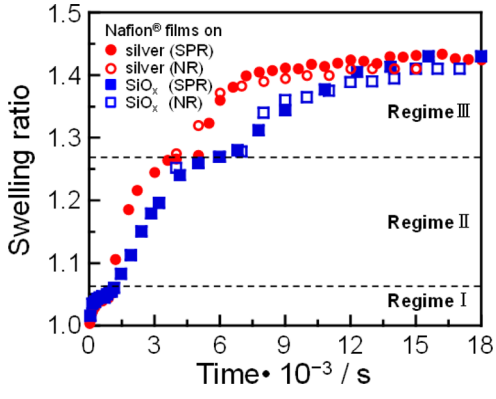

Figure 2. Time dependence of swelling ratio for Nafion films on silver (red) and SiO_x (blue) substrates with an h_0 of 47 and 49 nm, respectively, prior to coming in contact with water. The filled and open symbols are the data obtained SPR and neutron reflectivity measurements, respectively.

swelling ratio here is defined as the value of the film thickness in water (h_w) divided by h_0. Because the swelling ratio for the film became larger in water with increasing time, there is no doubt that water molecules were sorbed into the films in both cases. The thin Nafion films thickened in three steps named here as regimes I, II, and III. At first, the films asymptotically reached a swelling ratio of 1.05. Then, the films resumed thickening asymptotically up to 1.26. Finally, the swelling ratio reached 1.41. The corresponding data for thinner and thicker films are presented in Figure S2 of the Supporting Information. While the characteristic swelling ratio at the border between different regimes was neither dependent on the substrate species nor the film thickness, the swelling kinetics depended on the type of the substrate.

Dura and co-workers have reported that a water-containing multilamellar structure is formed in a Nafion film at the SiO_x interface and that a single hydrated layer is generated at the gold interface.[22] To examine the aggregation structure of our thin Nafion films near the substrate interface, NR measurements were conducted. In addition, NR analyses can verify our results obtained by SPR measurements.

Figure 3a and b show the NR curves for Nafion films with an h_0 of 53 nm supported on silver and quartz substrates,

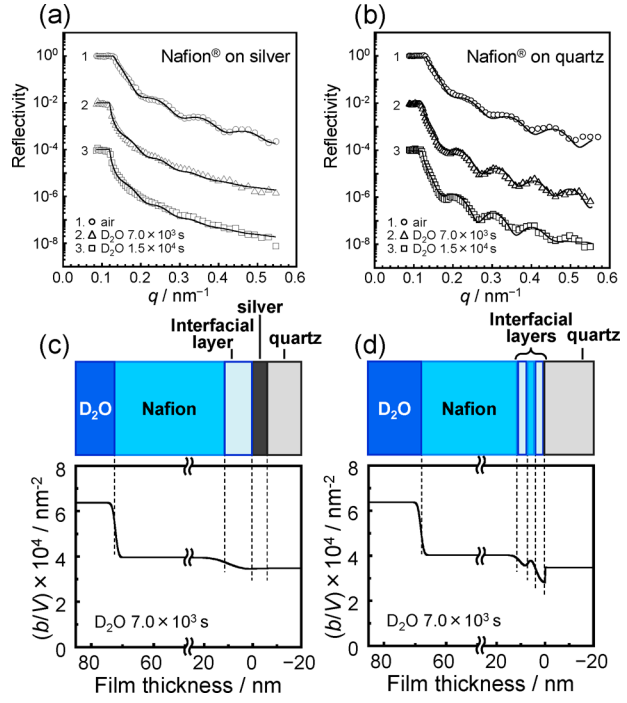

Figure 3. Neutron reflectivity curves for thin Nafion films with the original thickness (h_0) of 53 nm supported on (a) silver and (b) quartz substrates in air and D_2O. The curves are vertically offset for clarity. Experimental data sets are shown by symbols, and the best-fit curves calculated using the model (b/V) profiles shown in (c) and (d) are expressed by solid lines, respectively.

respectively, in air and D_2O at various given times. Here, D_2O was used instead of water because of two advantages. First, when neutron beams are guided to the Nafion film from the substrate side, a total reflection at the interface between D_2O and Nafion can be observed. This makes the analysis of NR profiles much easier. Second, the level of the background arising from the incoherent scattering can be reduced. The solid lines denote the best-fit calculated reflectivity to the

dx.doi.org/10.1021/mz400322q | ACS Macro Lett. 2013, 2, 856−859

experimental ones based on the model (b/V) profiles normal to the interface shown in Figure 3c and d, respectively. A model (b/V) profile with a moderately single hydrated interfacial layer was a suitable model of the Nafion film on the silver substrate. On the other hand, a model containing such an interfacial layer structure with the total thickness of about 15 nm also gave a better fitting for the film on the quartz substrate. The (b/V) values of two layers in the interfacial region were lower than that in the internal region of Nafion. This indicates that H_2O was sorbed in the interfacial region before soaking it into D_2O.[22] The swelling ratios evaluated from NR measurements are also plotted in Figure 2 and are consistent with the data from SPR measurements.

It has been accepted that the swelling of bulk Nafion by water sorption is accompanied by a structural change.[4−9] In short, the water first binds to sulfonic acid groups of the side chain portion of Nafion. When the water content in Nafion increases further, sphere-like ionic clusters are formed. The clusters finally connect to one another with the formation of bridges among the clusters. Interestingly, the swelling ratio for the structural transition, as noted in the introductory part, was coincident with the asymptotic swelling ratios in regimes I−III. Thus, the three-step sorption behavior shown in Figure 2 could be explained in terms of the structural evolution in the internal region of the film. Figure 4 shows a model for the swelling of a thin Nafion film. It is noteworthy that the hydrated layer is formed near the substrate.

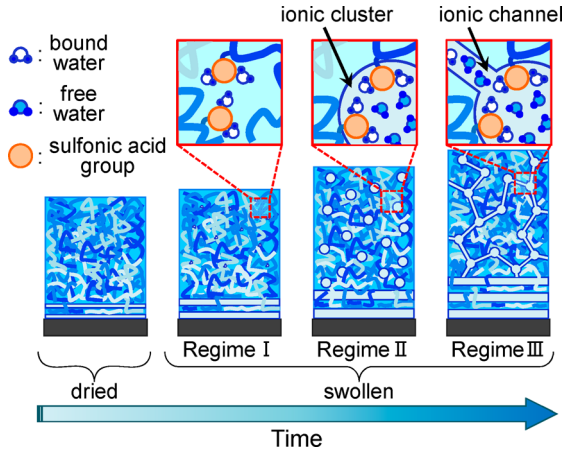

Figure 4. Schematic representation of the structural evolution in a thin Nafion film contacting water.

The thickness evolution of the film induced by water sorption as a function of time can be fitted by eq 1 based on a Fickian diffusion model,[23−25] allowing the evaluation of the diffusion coefficient of water into thin Nafion films in the regimes I, II, and III (D_I, D_{II}, and D_{III}), respectively.

$$\frac{h_w - h_{0,i}}{h_\infty - h_{0,i}} = 1 - \sum_{n=0}^{\infty}\left[\frac{8}{\{(2n+1)\pi\}^2}\right]\exp\left[-\{(2n+1)\pi\}^2\frac{D_i(t-t_{0,i})}{{h_{0,i}}^2}\right] \quad (1)$$

Here, the subscript i denotes the regime number and h_∞ and t_0 are the equilibrium film thickness and the starting time of regime i, respectively.

Figure 5 shows the h_0 dependence of the water diffusion coefficients in the thin Nafion films on the silver and SiO_x substrates. As a general trend for a given substrate, the diffusion coefficients were in the order of D_I, D_{III}, and D_{II}. In the regime

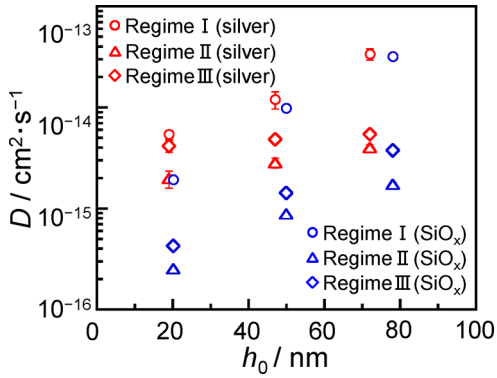

Figure 5. Diffusion coefficients (D_I, D_{II}, and D_{III}) of water into Nafion films on silver (red) and SiO_x (blue) substrates as a function of original film thickness.

I, water is sorbed into the homogeneous film. In the regimes II and III, at least, two diffusion mechanisms may exist; diffusion of waters bound on sulfonic acid groups of Nafion in the film and hopping diffusion of waters between sphere-like clusters. A similar discussion has been made for the self-diffusion of block copolymers in various microphase-separated structures.[26−29] In the case of the hopping diffusion, water molecules in a sphere-like cluster must diffuse into another by overcoming a thermodynamic barrier. This means that the hopping diffusion should be much slower than the diffusion obeying the former mechanism. Hence, the hopping diffusion mechanism would be more dominant in the regimes II. Besides, the diffusion was moderate in the regime III. Thus, in this regime, it seems most likely that the two diffusion mechanisms compete with each other.

The D_I, D_{II}, and D_{III} values are all smaller than the reported diffusion coefficient for the bulk material that is approximately 2.0×10^{-6} cm^2 s^{-1}.[23−25] The slowing down of water diffusion into the thin Nafion films can be explained in terms of the interfacial effect. In the case of the thin film, the ratio of the interface to the total volume of the film is quite large. In other words, physical properties of thin films can be controlled by the interface. This is the reason why water diffusion in the thin films slowed down. This is further validated in Figure 5 where the diffusion coefficient can be seen to decrease with decreasing thickness. The decrement at a particular thickness was more striking on the SiO_x substrate than on the silver one. This implies that the restriction of chain mobility is more marked for the SiO_x than for the silver. In the case of the silver substrate, the thickness effect became less important upon longer contact of the film with water, here defined by regimes II and III. This can be explained by the presence of water near the substrate[22,30] weakens the strong interaction between the side chain portion of Nafion and the hydroxy groups at the substrate. Taking into account that the amount of sorbed water increases with increasing time, the disappearance of the thickness effect can be also understood. On the other hand, the thickness effect remained important in regimes II and III. This is simply because the restriction of chain mobility should be more marked for the SiO_x substrate.

In conclusion, the water absorption kinetics and aggregation states in thin Nafion films were investigated by SPR and neutron reflectivity measurements. The water sorption behavior of thin Nafion films is divided into three regimes, which could be understood by using bulk system concepts, while its

dx.doi.org/10.1021/mz400322q | ACS Macro Lett. 2013, 2, 856−859

dynamics remarkably slows down due to the interaction between the substrate and Nafion and the confinement effect.

EXPERIMENTAL SECTION

As a material, Nafion, purchased from Sigma Aldrich Inc., was used. To evaluate the effect of the substrate on water absorption kinetics, silver-deposited quartz and glass substrates referred to as silver substrates, were employed. SiO_x substrates for SPR measurements were prepared by thermal deposition of SiO_x on the silver substrates. The surface chemistry of the SiO_x substrates is comparable to that of quartz substrates for NR measurements. Films with various thicknesses were prepared by spin-coating from Nafion alcohol dispersions onto the substrates. The films were dried under vacuum at 313 K for 24 h. The thickness of the Nafion films in a dried state was determined by ellipsometry to complement our discussion on the results of the SPR reflectivity measurement. The changes in thickness of the Nafion films in water were followed as a function of time by SPR and neutron reflectivity measurements. For SPR reflectivity measurements, visible light with a wavelength of 632.8 nm generated by a He−Ne laser was used as the light source for these measurements. The incident angle of the beam to the sample was defined as θ. A silicon photomultiplier detector was set at a position of 2θ. Hence, the reflectivity, which was defined as the intensity ratio of incident to detected beams, was measured under the specular condition as a function of θ. A liquid cell was mounted onto the film. Neutron reflectivity (NR) measurements were performed on Soft Interface Analyzer[31−33] (SOFIA; BL-16, Materials and Life Science Facility, Japan Proton Accelerator Research Complex, Tokai, Japan). A neutron beam was guided onto the film from the quartz side. NR profiles were then collected every 15 min after the films were immersed in D_2O. The analyses of NR profiles were carried out using the Parratt32 software based on Parratt's algorithm.[34] The (b/V) values for Nafion, the hydrophilic side chain portion of Nafion, quartz, silver, and the H_2O and D_2O used in these calculations were taken as 3.86×10^{-4}, 2.10×10^{-4}, 3.48×10^{-4}, 3.47×10^{-4}, -5.6×10^{-4}, and 6.37×10^{-4} nm^{-2}, respectively.

ASSOCIATED CONTENT

Supporting Information

Figure S1, Surface morphology of Nafion films in air and water; Figure S2, Swelling ratio for different-thick Nafion films. This material is available free of charge via the Internet at http://pubs.acs.org.

AUTHOR INFORMATION

Corresponding Author

*E-mail: k-tanaka@cstf.kyushu-u.ac.jp.

Notes

The authors declare no competing financial interest.

ACKNOWLEDGMENTS

We are grateful for helpful discussion with Prof. David P. Penaloza Jr., Keimyung University, and Dr. Yoshihisa Fujii, National Institute for Materials Science (NIMS). This research was partly supported by a Grant-in-Aid for Scientific Research (B; No. 24350061) from the Ministry of Education, Culture, Sports, Science and Technology, Japan. Neutron reflectivity measurements were performed on BL-16 at the Materials and Life Science Facility, J-PARC, Japan, under Program No. 2009S08.

REFERENCES

(1) Springer, T. E.; Zawodzinski, T. A.; Gottesfeld, S. *J. Electrochem. Soc.* **1991**, *138*, 2334−2342.
(2) Kreuer, K. D. *J. Membr. Sci.* **2001**, *185*, 29−39.
(3) Mauritz, K. A.; Moore, R. B. *Chem. Rev.* **2004**, *104*, 4535−4586.
(4) Yoshida, H.; Miura, Y. *J. Membr. Sci.* **1992**, *68*, 1−10.
(5) Laporta, M.; Pegoraro, M.; Zanderighi, L. *Phys. Chem. Chem. Phys.* **1999**, *1*, 4619−4628.
(6) Gebel, G.; Lambard, J. *Macromolecules* **1997**, *30*, 7914−7920.
(7) Gebel, G. *Polymer* **2000**, *41*, 5829−5838.
(8) Schmidt-Rohr, K.; Chen, Q. *Nat. Mater.* **2008**, *7*, 75−83.
(9) Hinatsu, J. T.; Mizuhata, M.; Takenaka, H. *J. Electrochem. Soc.* **1994**, *141*, 1493−1498.
(10) Jones, R. A. L.; Richards, R. W. *Polymers at Surfaces and Interfaces*; Cambridge University Press: Cambridge, U.K., 1999.
(11) Karim, A.; Kumar, S. *Polymer Surfaces, Interfaces and Thin Films*; World Scientific: Singapore, 2000.
(12) Tsui, O. K. C.; Russell, T. P. *Polymer Thin Films*; World Scientific: Singapore, 2008.
(13) Kanaya, T. *Glass Transition, Dynamics and Heterogeneity of Polymer Thin Films*; Springer: New York, 2013.
(14) Zhang, C.; Fujii, Y.; Tanaka, K. *ACS Macro Lett.* **2013**, *1*, 1317−1320.
(15) Krtil, P.; Trojánek, A.; Samec, Z. *J. Phys. Chem. B* **2001**, *105*, 7979−7983.
(16) Modestino, M. A.; Kusoglu, A.; Hexemer, A.; Weber, A. Z.; Segalman, R. A. *Macromolecules* **2012**, *45*, 4681−4688.
(17) Eastman, S. A.; Kim, S.; Page, K. A.; Rowe, B. W.; Kang, S.; Soles, C. L.; Yager, K. G. *Macromolecules* **2012**, *45*, 7920−7930.
(18) Modestino, M. A.; Paul, D. K.; Dishari, S.; Petrina, S. A.; Allen, F. I.; Hickner, M. A.; Karan, K.; Segalman, R. A.; Weber, A. Z. *Macromolecules* **2013**, *46*, 867−873.
(19) Knoll, W. *Annu. Rev. Phys. Chem.* **1998**, *49*, 569−638.
(20) Hori, K.; Matsuno, H.; Tanaka, K. *Soft Matter* **2011**, *7*, 10319−10326.
(21) http://www.mpip-mainz.mpg.de/documents/akkn/soft/index.html.
(22) Dura, J. A.; Murthi, V. S.; Hartman, M.; Satija, S. K.; Majkrzak, C. F. *Macromolecules* **2009**, *42*, 4769−4774.
(23) Yeager, H. L.; Steck, A. *J. Electrochem. Soc.* **1981**, *128*, 1880−1884.
(24) Majsztrik, P. W.; Satterfield, M. B.; Bocarsly, A. B.; Benziger, J. B. *J. Membr. Sci.* **2007**, *301*, 93−106.
(25) Hallinan, D. T.; Elabd, Y. A. *J. Phys. Chem. B* **2007**, *111*, 1520−6106.
(26) Lodge, T. P.; Dalvi, M. C. *Phys. Rev. Lett.* **1995**, *75*, 657−660.
(27) Hamersky, M. W.; Hillmayer, M. A.; Tirrell, M.; Bates, F. S.; Lodge, T. P.; Meerwall, E. D. *Macromolecules* **1998**, *31*, 5363−5370.
(28) Yokoyama, H.; Kramer, E. J.; Fredrickson, G. H. *Macromolecules* **2000**, *33*, 2249−2257.
(29) Yokoyama, H. *Mater. Sci. Eng., R* **2006**, *53*, 199−248.
(30) Wood, D. L.; Chlistunoff, J.; Majewski, J.; Borup, R. L. *J. Am. Chem. Soc.* **2009**, *131*, 18096−18104.
(31) Mitamura, K.; Yamada, N. L.; Sagehashi, H.; Seto, H.; Torikai, N.; Sugita, T.; Furusaka, M.; Takahara, A. *J. Phys.: Conf. Ser.* **2011**, *272*, 012017.
(32) Mitamura, K.; Yamada, N. L.; Sagehashi, H.; Torikai, N.; Arita, H.; Terada, M.; Kobayashi, M.; Sato, S.; Goko, S.; Furusaka, M.; Oda, T.; Hino, M.; Jinnai, H.; Takahara, A. *Polym. J.* **2013**, *45*, 100−108.
(33) Yamada, N. L.; Torikai, N.; Mitamura, K.; Sagehashi, H.; Sato, S.; Seto, H.; Sugita, T.; Goko, S.; Furusaka, M.; Oda, T.; Hino, M.; Fujiwara, T.; Takahashi, H.; Takahara, A. *Eur. Phys. J. Plus* **2011**, *126*, 108.
(34) http://www.hmi.de/bensc/instrumentation/instrumente/v6/refl/parratt_en.htm.